Numerical Analysis for the Dynamics of the Oxidation-Induced Stacking Fault in Czochralski-Grown Silicon Crystals

Jong Hoe Wang[†], Hyun Jung Oh and Hak-Do Yoo

R&D Center, LG Siltron Inc., 283 Imsoo-Dong, Kumi, Kyung-Buk 730-350, Korea
(*Received 18 July 2000 • accepted 7 November 2000*)

Abstract−The continuum model of point defect dynamics to predict the concentration of interstitial and vacancy is established by estimating expressions for the thermophysical properties of point defects and the point defect distribution in a silicon crystal and the position of oxidation-induced stacking fault ring (R-OiSF) created during the cooling of crystals in Czochralski silicon growth process are calculated by using the finite element analysis. Temperature distributions in the silicon crystal in an industrial Czochralski growth configuration are measured and compared with finite volume simulation results. These temperature fields obtained from finite volume analysis are used as input data for the calculation of point defect distribution and R-OiSF position. Calculations of continuum point defect distributions predict the transition between vacancy and interstitial dominated precipitations of microdefects as a function of crystal pull rate (V). The dependence of the radius of R-OiSF (R_{OiSF}) on the crystal length with fixed growth rate for a given hot zone configuration is examined. The R_{OiSF} is increased with the increase of crystal length. These predictions from point defect dynamics are well agreed with experiments and empirical V/G correlation qualitatively, where G is the axial temperature gradient at the melt/crystal interface.

Key words: Point Defect Dynamics, Oxidation-Induced Stacking Fault, Czochralski, Finite Element Method, Numerical Simulation

INTRODUCTION

The Czochralski crystal growth technique is the most widely used method for producing large silicon single crystals as substrates in the fabrication of electronic devices. The silicon wafers typically used in device fabrication are populated by distributions of microscopic precipitates, stacking faults and dislocation loops that result from the interactions of point defects - interstitials and vacancies - and impurities in the crystal during crystal growth, subsequent annealing of the crystal and device processing. Especially silicon crystals grown by Czochralski method are plagued by the appearance of oxidation-induced stacking faults ring (R-OiSF).

OiSF are plane defects generated in the surface region of silicon wafers during thermal oxidation process at typical temperature range between 900 and 1,200 °C. Although OiSF does not exist in as-grown crystals, their nuclei have already been formed during growth [Dornberger and Ammon, 1996]. The R-OiSF appears as an annular ring in which there is a high density of stacking faults after the silicon wafer is oxidized and etched. The OiSF distribution on a wafer surface after wet oxidation reflects the grown-in defect distribution of crystal and the R-OiSF separates a vacancy-rich inner and an interstitial-rich outer region of a wafer [Dornberger et al., 1997].

The radius of R-OiSF has been documented to be a function of the crystal pull rate (V) and the temperature field in the crystal during the crystal growth process [Hasebe et al., 1989; Ammon et al., 1995]. The faster the crystal pull rate, the larger the radius of the R-OiSF becomes and the closer to the crystal surface the R-OiSF ap-

proaches. Conversely, the slower the crystal pull rate, the smaller the R-OiSF radius, and, consequently, the R-OiSF moves nearer to the center of the crystal. When the crystal pull rate is further slowed down to a specific value, V_{crit}, the R-OiSF contracts toward the center of the crystal and disappears. The dependence of the R-OiSF on the crystal pull rate is shown schematically in Fig. 1.

The control of microscopic defects formed during crystal growth or subsequent anneal is one of the most important problems in the production of silicon wafer. It is well known that these defects have
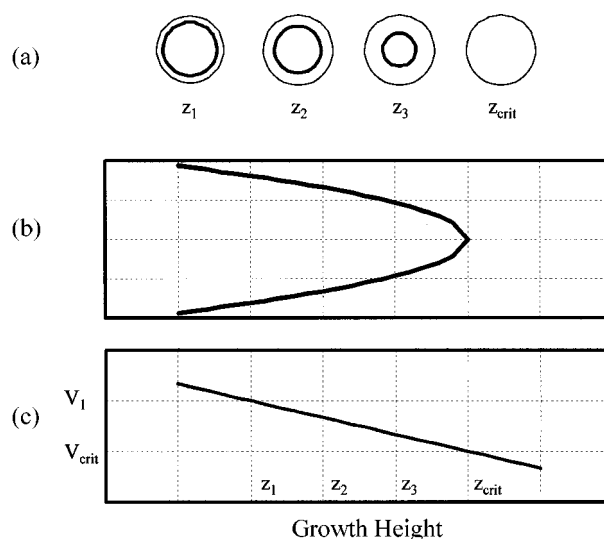
Fig. 1. Schematic diagram for the dependence of the R-OiSF on the crystal pull rate V. $V_1>V_2>V_3>V_{crit}$.
(a) OiSF on the wafer (b) an axial perspective of the R-OiSF and (c) the crystal pull rate.

[†]To whom correspondence should be addressed.
E-mail: wjha@lgsiltron.co.kr

effects on device performance inversely. In order to control microdefect formation the precise control of impurity and temperature distribution is required during growing, cooling, and annealing of the crystal. The thermal history of Czochralski silicon crystals has a dominating influence on the formation of microdefects [Dornberger and Ammon, 1996; Puzanov and Eidenzon, 1992; Wijaranakula, 1993].

Temperature field used in this work are taken directly from finite volume analysis of heat transfer in the crystal and throughout the Czochralski growth system for a particular hot zone configuration and growth rate. These temperature fields obtained from finite volume analysis are interpolated onto biquadratic finite element basis used for the defect concentrations and used as input in this work. The shape of the melt/crystal interface is calculated in the heat transfer analysis and is used to define the shape of the mesh in the point defect simulations.

Starting with Voronkov [1982], several models [Brown et al., 1994; Habu et al., 1993a, 1993b, 1993c, 1994; Sinno et al., 1997, 1998; Hu, 1985; Voronkov and Falster, 1998] have been presented to explain microdefect formation in silicon in terms of the dynamics of intrinsic point defect. The model of point defect dynamics includes point defect convection by crystal motion, diffusion by both Fickian and thermodiffusion driving force, and point defect recombination. This description of point defect dynamics is similar to the model proposed by Voronkov, Brown et al., Habu et al. and Sinno et al.

Voronkov's analysis [1982] described the transition between interstitial-related and vacancy-related defect regions in small-scale floating zone crystals. His approach gave V/G, where G is a characteristic temperature gradient at the melt/solid interface, as the critical parameter for determining whether vacancy or interstitial was in excess. Brown et al. [1994] describes the first step of an attempt to model the formation of microdefects by combining atomistic-level simulation of the equilibrium, transport, and kinetics of point defects and impurities in silicon with continuum modelling of defect transport and reaction. Their calculations of continuum point defect distribution predict the transition between vacancy and interstitial dominated precipitation of microdefects as a function of temperature gradient, crystal pull rate and crystal radius (0.63, 1.25, 2.50, 5.00 cm). These predictions are in qualitative agreement with experiments for FZ-grown crystals. Habu et al. [1993a, 1993b, 1993c, 1994] have assumed that point defect thermo-diffusion and radial transport play key roles in describing R-OiSF dynamics. Neglecting point defect recombination and solving the point defect equations numerically lead to a correlation of the R-OiSF location in terms of VG. Sinno et al. [1997, 1998] have presented and analyzed the model for the point defect dynamics in single crystal silicon. They used finite element simulation and asymptotic analysis to describe the appearance of the R-OiSF created during the cooling of silicon crystal in the Czochralski growth process. They gave a closed-form expression for the critical value of V/G for the location of the R-OiSF by using the asymptotic analysis of the point defect dynamics model.

The present paper focuses on the numerical analysis for the point defect dynamics and the position of the R-OiSF in Czochralski-grown single crystal silicon. The continuum model of point defect dynamics is established by estimating expressions for equilibrium,

transport and kinetic parameters and finite element analysis is performed to study the point defect distribution in a crystal and the position of the R-OiSF created during the cooling of silicon crystals in Czochralski growth process. The transition from interstitial to vacancy dominated precipitations of microdefects is studied numerically with the increase of the crystal pull rate. These predictions are compared qualitatively with the empirical V/G correlations. The dependence of the radius of R-OiSF (R_{OiSF}) on the crystal length at fixed growth rate for a given hot zone configuration is studied theoretically using the numerical simulation of the point defect dynamics for the first time. The results from point defect dynamics are in qualitative agreement with the experiment of Park et al. [1999].

MATHEMATICAL MODEL

The model equation to predict the point defect concentration is developed and shown in this section. Computed temperature distributions in the crystals were used as input for the calculation of thermophysical properties of I and V.

The continuum balance equations for the transport and interactions of vacancies and interstitials without accounting for the formation of aggregates are written in terms of concentration C_I and C_V (atoms/cm^3) as

$$\nabla \cdot \left(-D_I \nabla C_I + \frac{C_I D_I H_I^f}{kT^2} \nabla T \right) + V \frac{\partial C_I}{\partial z} + k_{IV}[C_I C_V - C_I^{eq} C_V^{eq}] = 0 \qquad (1)$$

$$\nabla \cdot \left(-D_V \nabla C_V + \frac{C_V D_V H_V^f}{kT^2} \nabla T \right) + V \frac{\partial C_V}{\partial z} + k_{IV}[C_I C_V - C_I^{eq} C_V^{eq}] = 0 \qquad (2)$$

where k_{IV} is the kinetic rate constant for the rate of recombination of vacancies and interstitials and C_I^{eq} (T) and C_V^{eq} (T) are the equilibrium concentrations of interstitials and vacancies, respectively, at the local temperature T of the crystal. D_I and D_V are the diffusion coefficients and H_I^f and H_V^f are the enthalpies of formation of the point defects and k is the Boltzmann constant. The defect concentration profiles are taken to be axisymmetric about the axis (z) of the crystal. The cylindrical co-ordinate system (r, z) is centered at the center of the melt/crystal interface. In a nonisothermal environment, point defects migrate both by Fickian diffusion through the crystal lattice and by thermodiffusion caused by the local temperature gradient.

Point defect concentrations in the crystal are predicted from Eqs. (1) and (2) with a specific set of boundary conditions on the crystal surfaces. We assume that the self-interstitial and vacancy concentrations are in equilibrium at the melt/crystal interface; this gives

$$C_I = C_I^{eq}(T_m), \qquad (3)$$

$$C_V = C_V^{eq}(T_m) \qquad (4)$$

The axis of the crystal (r=0) is taken as an axis of symmetry and we also assume that the flux of point defects is zero along the exposed crystal surface. The defect profiles are assumed to be in steady-state so that the time-dependence is neglected.

Other boundary conditions are possible. For example, Brown et al. [1994] and Habu et al. [1994] assume that point defect along the surface of the crystal are in equilibrium at the local temperature. Hu [1985] has proposed a Robin condition that lies between

the no-flux condition and the infinitely fast source/sink model, and Sinno et al. [1998] have examined the effects of equilibrium conditions at the crystal surface.

The OiSF subdivides the crystal into a self-interstitial rich outer region and vacancy rich inner region. A parameter $\Delta \equiv (C_I - C_V)/C_V^{eq}$ is defined, which is positive for the self-interstitial and negative for the vacancy dominated part of the crystal. The OiSF is assumed to occur at $\Delta=0$, where C_I is equal to C_V. The reason for the formation of a high density of stacking fault nuclei at $\Delta=0$ is still under discussion [Dornberger et al., 1997].

1. Thermophysical Properties of Point Defects

The continuum description of point defect dynamics is completed by supplying expressions for the equilibrium, transport and kinetic parameters. Estimating these parameters and their dependence on temperature is one of the most important components of modelling defect dynamics in silicon [Brown et al., 1994].

The thermophysical properties of point defects used in this analysis are

$$C_I^{eq}(T) = 3.945 \times 10^{26} \exp\left(-\frac{3.943 \text{ eV}}{kT}\right) \text{atoms/cm}^3, \quad (5)$$

$$D_I(T) = 2.101 \times 10^{-1} \exp\left(-\frac{0.907 \text{ eV}}{kT}\right) \text{cm}^2/\text{sec}, \quad (6)$$

$$C_V^{eq}(T) = 2.675 \times 10^{23} \exp\left(-\frac{2.848 \text{ eV}}{kT}\right) \text{atoms/cm}^3, \quad (7)$$

$$D_V(T) = 1.000 \times 10^{-4} \exp\left(-\frac{0.489 \text{ eV}}{kT}\right) \text{cm}^2/\text{sec} \quad (8)$$

Although the Gibbs free energy and enthalpies of formation of interstitials and vacancies depend on the temperature, only the mean values were used in the calculation presented here. The enthalpies of formation of interstitials (H_I^f) and vacancies (H_V^f) are used as 3.66 eV and 2.66 eV, respectively.

The kinetic constant k_{IV} is the last remaining parameter needed for specification of the defect dynamic model. The expression for a diffusion-limited process with a subsequent activation barrier for recombination is [Brown et al., 1994]

$$k_{IV}(T) = \frac{4\pi a_r}{\Omega c_s}(D_I + D_V)\exp\left(-\frac{\Delta G_{IV}}{kT}\right) \quad (9)$$

where $a_r = 10$ Å is the capture radius for recombination, $\Omega = 1/8a^3$ is the volume occupied by a host atom (a=5.53 Å for silicon) and $c_s = 5 \times 10^{22}$ atoms/cm³ is the lattice concentration of atoms. The free energy barrier for recombination $\Delta G_{IV} \equiv \Delta H_{IV} - T\Delta S_{IV}$ includes both enthalpic and entropic contributions from the recombination event. Unfortunately, there are no precise calculations of these contributions. The enthalpic barrier is used as $\Delta H_{IV} = 3.173$ eV and we use 15 k for ΔS_{IV}.

The thermophysical parameters were selected to minimize the difference between the results of defect dynamic analysis and the experimental measurements and predict quantitatively R_{OiSF} for a given hot zone configuration [Oh et al., 2000]. Although there is no rigorous method to estimate the optimum parameter set which enables to minimize the difference between the results of defect dynamic analysis and the experimental measurements, the objective function is used to quantify the goodness of fitting the thermophy-
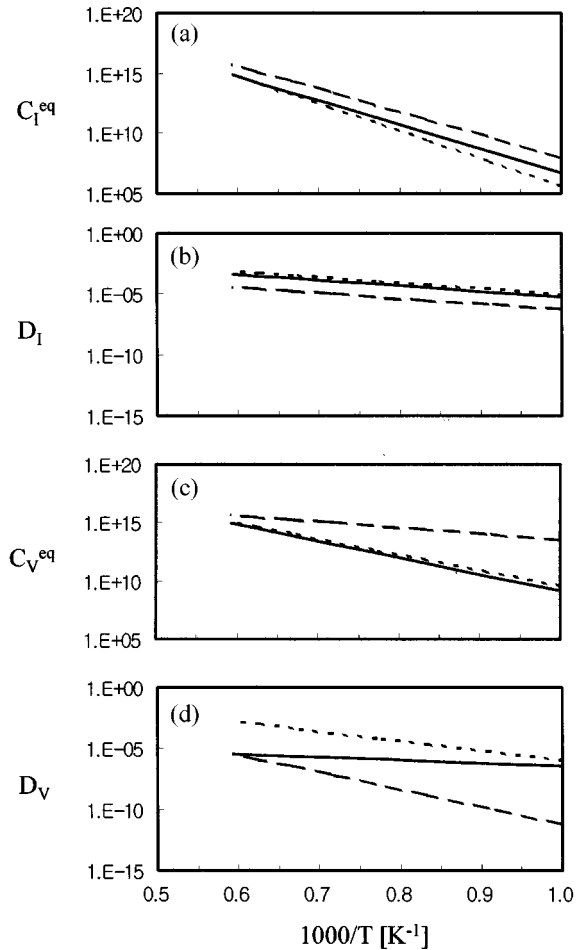
Fig. 2. Comparison of thermophysical properties to literature estimates. Solid line represents the value used in this work and the short and long dotted line are literature estimates in references [Habu and Tomiura, 1996; Zimmermann and Ryssel, 1992], respectively.

sical properties to experimental data. The objective function (Λ) is as follows

$$\Lambda \equiv \frac{1}{n}\sqrt{\sum_{i=1}^{n}[R_{OiSF}(V_i) - R_{OiSF}^{experiment}(V_i)]^2} \quad (10)$$

where $\{V_i\}$ is a set of crystal pull rates within a range for which R-OiSF is observed experimentally. The values of the equilibrium, transport and kinetic constants described above are compared in Fig. 2 with those from the literature [Habu and Tomiura, 1996; Zimmermann and Ryssel, 1992]. The mathematically elliptic balance equations with boundary conditions are solved numerically.

NUMERICAL ANALYSIS

In many materials processing technologies like casting and crystal growth, the process are controlled by heat transfer in complex geometry. The computer code STHAMAS is designed to be used as a tool for the analysis of heat transfer problems in crystal growth configurations. STHAMAS stands for Stress, Heat and mass Transfer Analysis using a Multigrid Accelerated Solver.

Temperature distributions in growing Czochralski crystals and in a given hot zone assembly for various growth conditions were calculated by employing the finite volume code STHAMAS in order to establish a quantitative model for the dependence of OiSF diameter on pull speed and crystal length. These temperature fields are used as input in the point defect simulations.

Dornberger et al. [1997] measured the temperature within an industrial Czochralski silicon puller and compared with simulation results. The temperature distribution of the furnace was computed with three different software codes; FEMAG, STHAMAS, IHTCM. They have demonstrated that these models can be used to predict the temperature distribution of growing silicon crystals in the case of Czochralski growth configuration, by exception of the melt convection problem, which has not yet been satisfactorily solved.

Based on the symmetric condition, the code takes into account heat transfer by conduction in solid parts and radiative heat transfer in furnace enclosures. The schematic drawing of thermocouples measurement are shown in Fig. 3(a). Computed temperatures were verified in Fig. 3(b) by comparison with thermo-couple measurements in crystals. Fig. 3(b) shows the validity of the predictied temperature distrinutions in silicon crystal phase. Radial variations of the axial temperature gradients, $G(r)$, at the crystal/melt interface in the growing crystals were determined from computed temperature
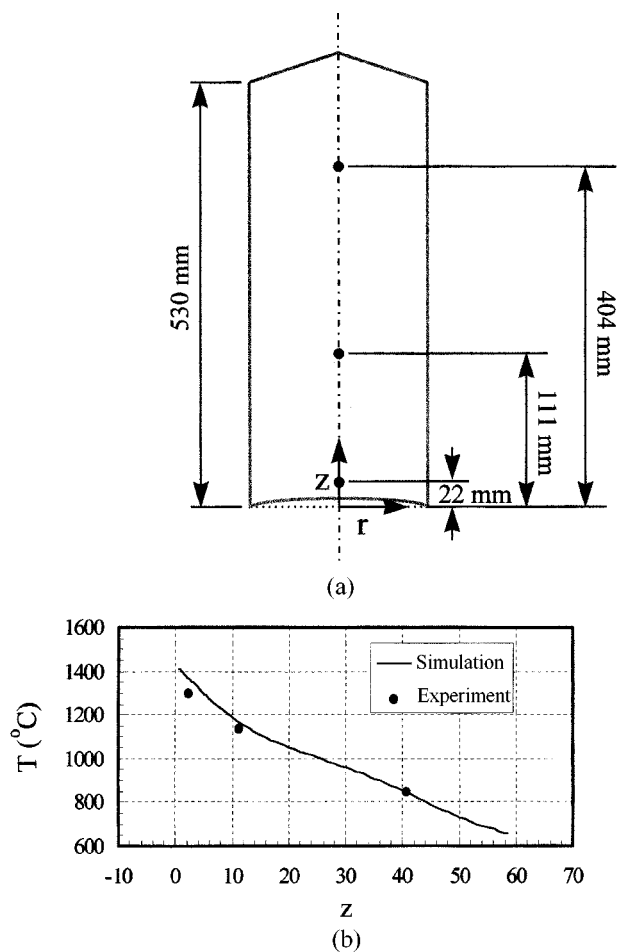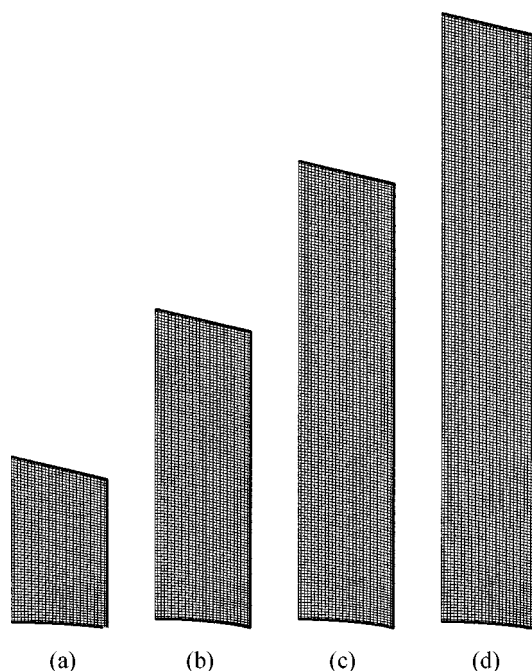

Fig. 4. Typical mesh shape used in the numerical Analaysis for the distributions of vacancies and interstitials.
(a) 20 cm, (b) 40 cm, (c) 60 cm, and (d) 80 cm crystal length.
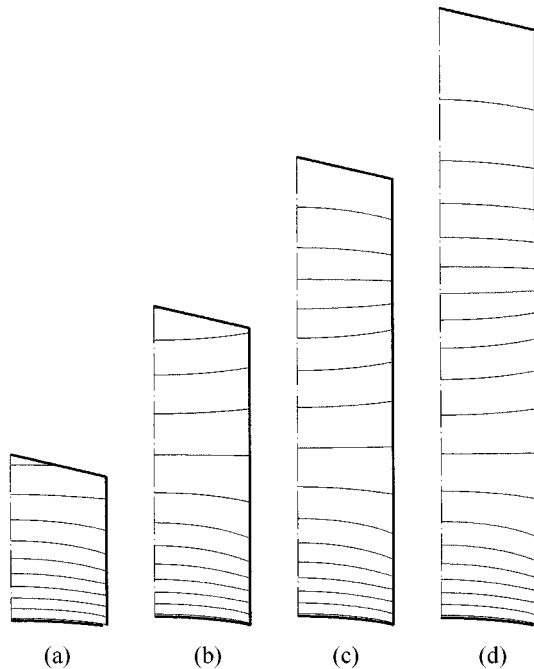
distributions.

The finite element method is used for discretization of the complete set of the mathematical model. The concentration fields are represented in expansions of Lagrangian biquadratic basis functions. A mesh is formed of quadrilateral elements which span the compuational domains corresponding to the crystal phase. Sample meshes are shown in Fig. 4. The field equations are put into the weak form and boundary conditions are imposed in the normal manner [Wang et al., 1996; Na et al., 1995].

The nonlinear algebraic equations set is linearized by Newton-Raphson method. All unknowns are obtained simultaneously using the Newton iteration scheme. All the contribution to the Jacobian matrix are computed in closed form. Numerical nine-point Gaussian quadrature for volume integrals and three-point Gaussian quadrature for the surface integrals are used to calculating the residual equations and Jacobian matrix. A frontal solution algorithm [Hood, 1976] was employed to solve the entire set of linear equations and minimize the core memory.
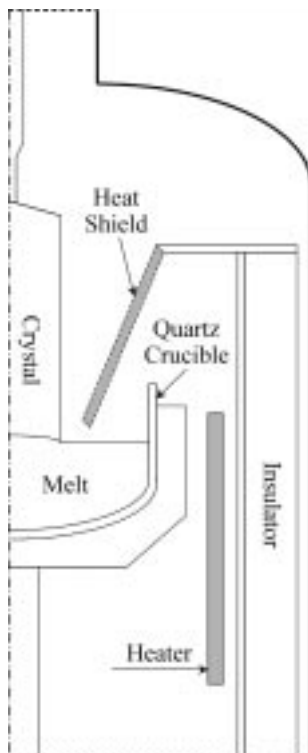
RESULTS AND DISCUSSIONS

The interstitial and vacancy concentration fields in the silicon crystal phase was obtained by applying the numerical method to the mathematical model for the growth of 200 mm silicon single crystal in a given hot zone configuration. The effects of crystal pull rate and crystal length on the location of R-OiSF was investigated numerically.

The temperature fields in the crystal phase at several crystal length are shown in Fig. 5 for calculations at crystal pull rates of 0.6 mm/min. The thermal surrounding of the crystal such as heat shield and hot zone configurations is shown schematically in Fig. 6. The in-

(a)

(b)

Fig. 3. (a) Schematic drawing of thermocouples measurement and (b) computed and measured temperature in crystal phase.
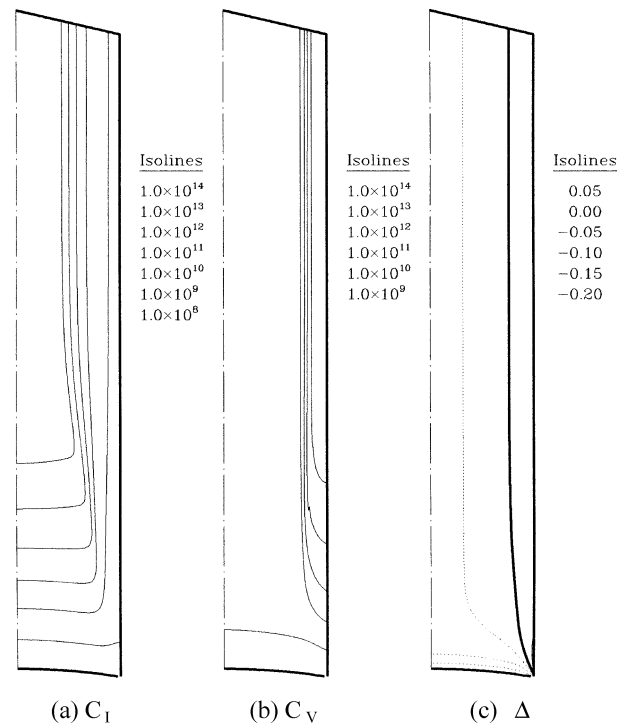
Fig. 5. Predicted temperature distributions of 200 mm crystal growth system.
(a) 20 cm, (b) 40 cm, (c) 60 cm, and (d) 80 cm crystal length. The spacing of the isotherms is 50 K and the thick line represents the melt/crystal interface isotherm at 1,685 K.

(a) C_I (b) C_V (c) Δ

Fig. 7. Sample profiles of (a) interstitial, C_I, (b) vacancy concentrations, C_V fields and (c) relative super-saturation, Δ for V=0.6 mm/min and crystal length of 80 cm.

of 80 cm. General characteristics of these results are typical for point defect dynamics in silicon. The gradient of the point defect concentration is steeper axially near the melt/crystal interface, and the point defect distributions are effectively frozen as shown by the contours for C_I, C_V and Δ. The variation of the contour Δ=0 emphasizes the competition between interstitial and vacancy for dominance in the crystal. The interesting feature of this field is the transition in radial direction between an excess of vacancy (Δ<0) in the crystal core and an excess of interstitial (Δ>0) in an annular ring around the crystal surface.

1. Effects of Crystal Pull Rate

Increasing the crystal pull rate at fixed crystal length simply causes

Fig. 6. The schematic drawing of hot zone configurations in a silicon Czochralski crystal growth furnace.

terstitial and vacancy concentration fields and contours of Δ are shown in Fig. 7 at crystal pull rates of 0.6 mm/min and crystal length
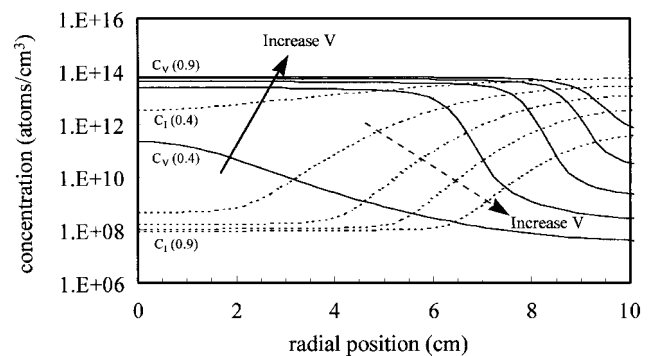

Fig. 8. Radial variation of interstitial and vacancy concentration in a silicon single crystal for different pull rates. Solid and dotted lines represent C_V and C_I, respectively. The range of crystal pull rate is between 0.4 and 0.9 mm/min and the increase of V is 0.1 mm/min.
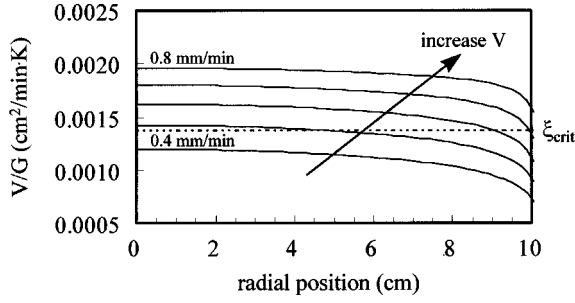
Fig. 9. V/G as a function of r for crystal pull rate from 0.4 to 0.9 mm/min with 0.1 mm/min spacing. The dotted line represents ξ_{crit}.

the crystal to move more rapidly through a certain temperature range and lessons the effects of radial diffusion. The effects of the crystal pull rate on the concentrations of interstitial and vacancy and the location of R-OiSF are shown in Fig. 8. The concentrations of point defect in the figure are the values at the top of the crystal. The fully developed profile of C_I and C_V in axial direction makes it convenient to represent the results in terms of the radial variation of the defect concentrations at the top of the crystal. Such results for a different crystal pull rate demonstrate the growth of the region of excess vacancy from a crystal dominated by interstitial with increasing V.

At lower crystal pull rate (e.g. V=0.4 mm/min at the crystal length of 80 cm in a given hot zone configuration), interstitial is in excess everywhere. And vacancy is in excess at higher crystal pull rate (e.g. 0.8 mm/min). These results are in qualitative agreement with the predictions of empirical V/G correlation as shown in Fig. 9. The axial temperature gradient at the melt/crystal interface, G, is defined as $G(r) \equiv -[\partial T/\partial z]_{\partial D_I}$, where ∂D_I represents the boundary for the melt/crystal interface. According to the experimental findings [Dornberger and Ammon, 1996], it can be assumed that vacancy-type defects are formed if V/G>ξ_{crit}, and interstitial-type defects will dominates for V/G<ξ_{crit}. In this work, the specific value for the critical V/G (ξ_{crit}) is used as 1.38×10^{-3} cm^2/min·K [Sinno et al., 1997].

2. Effects of Crystal Length

Park et al. [1999] have studied the effects of pulling rate fluctuation on the vacancy-interstitial boundary formation in Czochralski silicon single crystal growth, and they explained the gradual increase of R_{OiSF} as the decrease of temperature gradient during the crystal growth process. The effects of crystal length on the axial temperature gradient at melt/crystal interface and the location of R-OiSF were observed at a fixed crystal length in a given hot zone assembly. The decrease of G with the increase of crystal length in a given hot zone assembly may be caused by the addition of the heated zone in the crystal phase due to the radiation from the melt and the upper part of the heater as shown in Fig. 5.

The effects of the crystal length on the concentrations of interstitial and vacancy are shown in Fig. 10(a). The R_{OiSF} predicted in this work is shown together with the results of empirical V/G analysis in Fig. 10(b). The R_{OiSF} is increased with the increase of crystal length at a fixed crystal pull rate in a fixed hot zone configuration. The results from point defect dynamics are in qualitative agreement with the predictions of empirical V/G correlation and the experi-
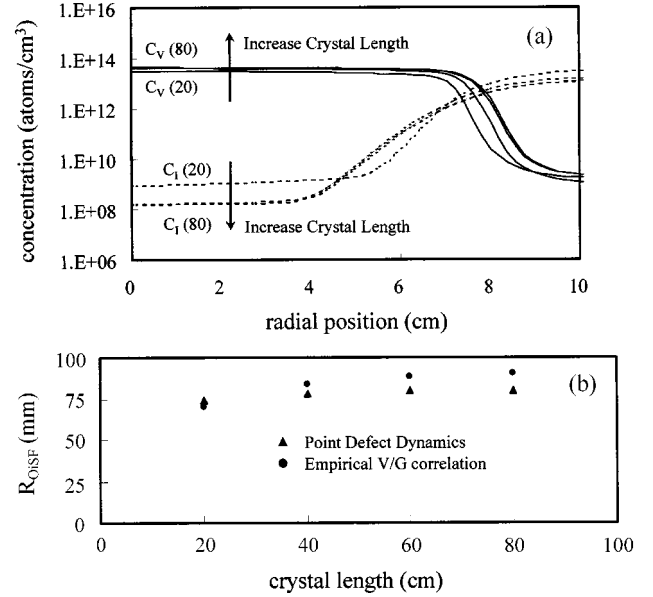

Fig. 10. The effects of crystal length on (a) the radial variation of interstitial and vacancy concentration and (b) the radius of R-OiSF, R_{OiSF}.

ment of Park et al. [1999].

CONCLUSIONS

The mathematical model of point defect dynamics has been developed to study the concentration of point defects by supplying expression for equilibrium, transport and kinetic parameters. Temperature fields used in this work are taken from finite volume analysis of heat transfer in the crystal and throughout the industrial Czochralski growth system for a particular hot zone configuration and growth rate. These temperature fields are compared with thermocouple measurements in crystal and used as input. With finite element analysis, the point defect distribution and the position of R-OiSF are studied.

The numerical computations give a detailed picture of the development of the self-interstitial and vacancy distributions in a silicon single crystal during the cooling of crystals in Czochralski growth. Simulation results for a several crystal pull rate demonstrate the growth of the region of excess vacancy from a crystal dominated by interstitial with increasing V, and interstial is in excess everywhere at lower crystal pull rate. The R_{OiSF} is increased with the increase of crystal length at a fixed V in a fixed hot zone configuration. The predictions from point defect dynamics are in qualitative agreement with experiments and empirical V/G analysis when correlated with the location of the R-OiSF. This work will give the basis for direct comparison between simulation and the observation of microdefect distributions in Czochralski-grown silicon wafers.

NOMENCLATURE

a_r : capture radius of recombination [Å]
C_I : concentrations of interstitials [atoms/cm^3]
C_V : concentrations of vacancies [atoms/cm^3]
C_I^{eq} : equilibrium concentrations of interstitials [atoms/cm^3]

C_V^{eq} : equilibrium concentrations of vacancies [atoms/cm^3]

c_s : lattice concentration of atoms [atoms/cm^3]

D_I : diffusion coefficient of interstitials [cm^2/sec]

D_V : diffusion coefficient of vacancies [cm^2/sec]

G : axial temperature gradient at the melt/crystal interface [K/cm]

H_I^f : enthalpies of formations of interstitials [eV]

H_V^f : enthalpies of formations of vacancies [eV]

k : Boltzmann constant [J/K]

k_{IV} : kinetic rate constant for the rate of recombination of vacancies and interstitials [cm^3/atoms·sec]

r : radial coordinate [cm]

R_{OiSF} : radius of oxidation-induced stacking faults ring [cm]

T : temperature [K]

T_m : melting temperature of silicon [K]

V : crystal pull rate [mm/min]

V_{crit} : critical crystal pull rate [mm/min]

z : axial coordinate [cm]

z_{crit} : critical growth height [cm]

Greek Letters

Δ : characteristic parameter defined as $\Delta \equiv (C_I - C_V)/C_V^{eq}$ [·]

Ω : volume occupied by a host atom [Å^3]

ΔG_{IV} : Gibbs free energy barrier for recombination [eV]

ΔH_{IV} : enthalpic energy barrier for recombination [eV]

ΔS_{IV} : entropic contributions from the recombination event [eV/K]

ξ_{crit} : critical value of V/G to predict the location of the position of OiSF [cm^2/min·K]

REFERENCES

Ammon, W., Dornberger, E., Oelkrug, H. and Weidner, H., "The Dependence of Bulk Defects on the Axial Temperature Gradient of Silicon Crystals during Czochralski Growth," *J. Cryst. Growth*, **151**, 273 (1995).

Brown, R. A., Maroudas, D. and Sinno, T., "Modelling Point Defect Dynamics in the Crystal Growth," *J. Cryst. Growth*, **137**, 12 (1994).

Dornberger, E. and Ammon, W., "The Dependence of Ring-Like Distributed Stacking Faults on the Axial Temperature Gradient of Growing Czochralski Silicon Crystals," *J. Electrochem. Soc.*, **143**, 1648 (1996).

Dornberger, E., Gräf, D., Suhren, M., Lambert, U., Wagner, P., Dupret, F. and Ammon, W., "Influence of Boron Concentration on the Oxidation-induced Stacking Fault Ring in Czochralski Silicon Crystals," *J. Cryst. Growth*, **180**, 343 (1997).

Dornberger, E., Tomzig, E., Seidl, A., Schmitt, S., Leister, H.-J., Schmitt, Ch. and Müller, G., "Thermal Simulation of the Czochralski Silicon Growth Process by Three Different Models and Comparison with Experimental Results," *J. Cryst. Growth*, **180**, 461 (1997).

Habu, R., Yunoki, I., Saito, T. and Tomiura, A., "Diffusion of Point Defects in Silicon Crystals during Melt-growth. I. Uphill Diffusion," *Jpn. J. Appl. Phys.*, **32**, 1740 (1993).

Habu, R., Kojima, K., Harada, H. and Tomiura, A., "Diffusion of Point Defects in Silicon Crystals during Melt-growth. II. One Diffusion Model," *Jpn. J. Appl. Phys.*, **32**, 1747 (1993).

Habu, R., Kojima, K., Harada, H. and Tomiura, A., "Diffusion of Point Defects in Silicon Crystals during Melt-growth. III. Two Diffusion Model," *Jpn. J. Appl. Phys.*, **32**, 1754 (1993).

Habu, R., Iwasaki, T., Harada, H. and Tomiura, A., "Diffusion Behavior of Point Defects in Si Crystal during Melt-Growth. IV. Numerical Analysis," *Jpn. J. Appl. Phys.*, **33**, 1234 (1994).

Habu, R. and Tomiura, A., "Distribution of Grown-in Crystal Defects in Silicon Crystals Formed by Point Defect Diffusion during Melt-Growth: Disappearance of the Oxidation Induced Stacking Faults-Ring," *Jpn. J. Appl. Phys.*, **35**, 1 (1996).

Hasebe, M., Takeoka, Y., Shinoyama, S. and Naito, S., "Formation Process of Stacking Faults with Ringlike Distribution in CZ-Si Wafers," *Jpn. J. Appl. Phys.*, **28**, L1999 (1989).

Hood, P., "Frontal Solution Program for Unsymmetric Matrices," *Int. J. Num. Meth. Eng.*, **10**, 379 (1976).

Hu, S. M., "Interstitial and Vacancy Concentrations in the Presence of Interstitial Injection," *J. Appl. Phys.*, **57**, 1069 (1985).

Na, S. Y. and Kim, D. H., "Three-dimensional Modelling of Non-newtonian Fluid Flow in a Coat-hanger Die," *Korean J. Chem. Eng.*, **12**, 236 (1995).

Oh, H. J., Wang, J. H. and Yoo, H.-D., "Comparison of Numerical Simulation and Experiment for the OiSF-ring Diameter in Czochralski-growth Silicon Crystal," (2000) Preparation.

Park, B. M., Seo, G. H. and Kim, G., "Effects of Pulling Rate Fluctuation on the Interstitial-vacancy Boundary Formation in CZ-Si Single Crystal," *J. Cryst. Growth*, **203**, 67 (1999).

Puzanov, N. I. and Eidenzon, A. M., "The Effect of Thermal History during Crystal Growth on Oxygen Precipitation in Czochralski-grown Silicon," *Semicond. Sci. Technol.*, **7**, 406 (1992).

Sinno, T., Brown, R. A., Ammon, W. and Dornberger, E., "On the Dynamics of the Oxidation-induced Stacking Fault Ring in as-grown Czochralski Silicon Crystals," *Appl. Phys. Lett.*, **70**, 2250 (1997).

Sinno, T., Brown, R. A., Ammon, W. and Dornberger, E., "Point Defect Dynamics and the Oxidation-induced Stacking-fault Ring in Czochralski-grown Silicon Crystals," *J. Electrochem. Soc.*, **145**, 302 (1998).

Voronkov, V. V., "The Mechanism of Swirl Defects Formation in Silicon," *J. Cryst. Growth*, **59**, 625 (1982).

Voronkov, V. V. and Falster, R., "Vacancy-type Microdefect Formation in Czochralski Silicon," *J. Cryst. Growth*, **194**, 76 (1998).

Wang, J. H., Kim, D. H. and Chung, D.-S., "Analysis of Moving Boundary Problem of Growth of Bismuth Germanate Crystal by Heat Exchanger Method," *Korean J. Chem. Eng.*, **13**, 503 (1996).

Wijaranakula, W., "Real-time Simulation of Point Defect Reactions Near the Solid and Melt Interface of a 200 mm Diameter Czochralski Silicon Crystal," *J. Electrochem. Soc.*, **140**, 3306 (1993).

Zimmermann, H. and Ryssel, H., "Gold and Platinum Diffusion: The Key to the Understanding of Intrinsic Point Defect Behavior in Silicon," *Appl. Phys. A*, **55**, 121 (1992).